



## ORIGINAL ARTICLE

# Microstructure and mechanical properties of geopolymers with different dolomitic lime contents

## *Microestrutura e propriedades mecânicas de geopolímeros com diferentes teores de cal dolomítica*

Allan Guimarães Borçato<sup>a,b</sup> Neusa Aparecida Munhak Beltrame<sup>a</sup> Tassiane Apolinário de Oliveira<sup>a</sup> Ronaldo Alves de Medeiros-Junior<sup>a</sup> <sup>a</sup>Universidade Federal do Paraná – UFPR, Programa de Pós-graduação em Engenharia Civil – PPGEC, Curitiba, PR, Brasil<sup>b</sup>Instituto Federal de Santa Catarina – IFSC, Departamento Acadêmico de Construção Civil – DACC, Florianópolis, SC, Brasil

Received 27 December 2023

Revised 6 March 2024

Accepted 8 March 2024

**Abstract:** This study investigated the effect of dolomitic lime incorporation on the microstructure and mechanical properties of metakaolin-based geopolymers activated by alkaline solution. Five geopolymer mixtures were prepared with the addition of 0.0%, 2.5%, 5.0%, 7.5%, and 10.0% dolomitic lime. The microstructure of the geopolymers was evaluated by scanning electron microscopy (SEM), energy-dispersive X-ray spectroscopy (EDS), and X-ray diffraction analyses (XRD). The compressive strength of the mixtures ranged between 53.2 and 63.0 MPa after 28 days of ambient curing. SEM/EDS analyses showed that the main phases formed were the N-A-S-H gel together with the C-A-S-H and N-M-A-S-H gels in the mixtures with dolomitic lime. In summary, the results showed that the incorporation of dolomitic lime can significantly improve the microstructure and properties of geopolymers.

**Keywords:** geopolymer, metakaolin, dolomitic lime, magnesium hydroxide, calcium hydroxide.

**Resumo:** Este estudo investigou o efeito da incorporação de cal dolomítica na microestrutura e nas propriedades mecânicas de geopolímeros à base de metacaulim ativados por solução alcalina. Foram preparadas cinco misturas de geopolímeros com adição de 0,0%, 2,5%, 5,0%, 7,5% e 10,0% de cal dolomítica. A microestrutura dos geopolímeros foi avaliada por microscopia eletrônica de varredura (MEV), espectroscopia de energia dispersiva de raios X (EDS) e análises de difração de raios X (DRX). A resistência à compressão das misturas variou entre 53,2 e 63,0 MPa após 28 dias de cura ambiente. As análises SEM/EDS mostraram que as principais fases formadas foram o gel N-A-S-H juntamente com os géis C-A-S-H e N-M-A-S-H nas misturas com cal dolomítica. Em resumo, os resultados mostraram que a incorporação de cal dolomítica pode melhorar significativamente a microestrutura e as propriedades dos geopolímeros.

**Palavras-chave:** geopolímero, metacaulim, cal dolomítica, hidróxido de magnésio, hidróxido de cálcio.

**How to cite:** A. G. Borçato, N. A. M. Beltrame, T. A. Oliveira, and R. A. Medeiros-Junior, “Microstructure and mechanical properties of geopolymers with different dolomitic lime contents,” *Rev. IBRACON Estrut. Mater.*, vol. 18, no. 1, e18101, 2025, <https://doi.org/10.1590/S1983-41952025000100001>

## 1 INTRODUCTION

Geopolymers are inorganic polymers formed by a polymerization reaction between an aluminosilicate source and an activator solution [1]. The main aluminosilicate sources used in the production of geopolymers are fly ash [2]–[4] and metakaolin [5]–[7]. In addition, other materials such as bottom ash, natural zeolites, palm oil fuel ash, rice husk ash, biomass fly ash, and silico-manganese fume have also been evaluated as sources of aluminosilicates [8].

**Corresponding author:** Allan Guimarães Borçato. E-mail: [borcato.allan@gmail.com](mailto:borcato.allan@gmail.com)

**Financial support:** None.

**Conflict of interest:** Nothing to declare.

**Data Availability:** The data that support the findings of this study are available from the corresponding author, [A.G.B.], upon reasonable request.



This is an Open Access article distributed under the terms of the Creative Commons Attribution License, which permits unrestricted use, distribution, and reproduction in any medium, provided the original work is properly cited.

Several studies have evaluated the properties of geopolymers, mainly because of their potential to provide a sustainable waste disposal solution since the sources of aluminosilicates are usually residual by-products of an industrial process or materials whose production has a lower environmental impact than the production of Portland cement [9], [10]. In addition, geopolymers can have good mechanical properties and good resistance to aggressive environments [11], [12]. All these aspects make geopolymers a potential candidate for field use in civil engineering, automotive, waste management, and retrofitting of existing buildings [8], [13].

Although metakaolin has significant reactive contents of silica and alumina in its chemical composition [14], the percentage of calcium in its chemical composition is practically negligible [15], [16]. From the evaluation of the chemical composition of different types of metakaolin obtained in several studies and in several countries for the production of geopolymers, Jindal et al. [15] found that the average value of calcium (CaO) contained in metakaolin is about 0.2% by mass. Thus, several researchers aim to evaluate the effects of calcium incorporation in metakaolin-based geopolymers, because calcium incorporation can promote an increase in mechanical strength due to the formation of C-S-H and C-A-S-H gels in the geopolymer matrix [5], [7], [17]–[19]. The incorporation of calcium compounds can also show significant benefits to the mechanical properties of geopolymers prepared from different aluminosilicate sources [2], [4], [20]–[22]. Huo et al. [23] identified from machine learning models that the molar ratio of  $\text{SiO}_2/\text{CaO}$  in geopolymers is one of the five most important parameters influencing the compressive strength of geopolymers.

Calcium incorporation is usually realized by adding CaO [2] or  $\text{Ca}(\text{OH})_2$  [2], [4], [5], [17], [20]–[22] to the geopolymer preparation. However, the addition of  $\text{Ca}(\text{OH})_2$  is more advantageous than CaO. This is because the addition of  $\text{Ca}(\text{OH})_2$  results in the formation of C-S-H and C-A-S-H gels in the geopolymer matrix and at the same time contributes to the better dissolution of the precursor due to the increased alkalinity of the medium, which consequently contributes to the geopolymerization [2]. Similar to the findings of Temuujin et al. [2], Chen et al. [19] found that the incorporation of calcium hydroxide increased the dissolution of the precursor.

Exploring the effect of  $\text{Ca}(\text{OH})_2$  on the product gel of fly ash-based pastes activated by an alkaline activator, Zhao et al. [22] identified that the incorporation of high  $\text{Ca}(\text{OH})_2$  contents can result in the higher forms of C-A-S-H and C-S-H gels than N-A-S-H and C, N-A-S-H gels. This contributed to the increased compressive strength due to the densification of the matrix. Similarly, Temuujin et al. [2] noted that the addition of CaO and  $\text{Ca}(\text{OH})_2$  to fly ash-based geopolymers resulted in the formation of C-S-H and C-A-S-H gels. After the addition of 3%  $\text{Ca}(\text{OH})_2$ , the compressive strength at 7 days of age increased from 11.8 MPa to 29.2 MPa in geopolymers cured at ambient temperature. Yang et al. [4] also evaluated the effect of  $\text{Ca}(\text{OH})_2$  addition on the mechanical properties of fly ash-based geopolymers. The authors concluded that increasing the level of the  $\text{Ca}(\text{OH})_2$  addition promoted an increase in the compressive strength due to the increased densification of the microstructure. The compressive strength of the mixture with 19% of  $\text{Ca}(\text{OH})_2$  addition was 210% higher than the compressive strength of the mixture with 4% addition, reaching 29.3 MPa in 28 days. Kim et al. [7] also observed that the addition of  $\text{Ca}(\text{OH})_2$  resulted in superior mechanical properties in metakaolin-based geopolymers. Lv et al. [24] observed that the addition of  $\text{Ca}(\text{OH})_2$  to fly ash and metakaolin-based geopolymers can significantly improve the compressive strength.

In summary, the incorporation of  $\text{Ca}(\text{OH})_2$  is beneficial to the mechanical properties of geopolymers because it contributes to the formation of C-S-H and C-A-S-H gels due to its availability in the material matrix [2], [4], [5], [7], [17]–[22], [25]. This results in improved mechanical properties due to the refinement and compaction of the geopolymer matrix caused by the formation of C-S-H and C-A-S-H gels [23]. However, the use of high-purity  $\text{Ca}(\text{OH})_2$  is expensive. Therefore, the use of commercial hydrated lime of calcitic origin is a viable option for this process. However, in several regions, it is not possible to obtain hydrated lime of calcitic origin, because, from the natural mineral formations, it is only possible to obtain hydrated lime of dolomitic origin, which is a material with high magnesium content.

Therefore, since there are no studies reported in the literature on the use of dolomitic lime in the production of geopolymers, this research aimed to evaluate the effects of incorporating dolomitic lime on the mechanical properties and microstructure of metakaolin-based geopolymers. The objective of this study is to understand whether the use of lime with a different origin (dolomitic) can also add good properties to the geopolymer, which reinforces the innovation of this article since there are no previous reports with this approach.

## 2 MATERIALS AND METHODS

### 2.1 Materials

#### 2.1.1 Raw materials

The metakaolin (MK) and dolomitic lime (DL) were commercially purchased. Table 1 shows the chemical composition of MK and DL determined by X-ray fluorescence (XRF) analysis. The loss on ignition (LOI) in Table 1 was determined by mass loss up to 1000 °C.

**Table 1.** Chemical composition in % mass of MK and DL.

Oxides	SiO <sub>2</sub>	Al <sub>2</sub> O <sub>3</sub>	CaO	MgO	Fe <sub>2</sub> O <sub>3</sub>	K <sub>2</sub> O	SO <sub>3</sub>	TiO <sub>2</sub>	P <sub>2</sub> O <sub>5</sub>	Na <sub>2</sub> O	LOI
MK	64.44	28.76	0.22	0.22	1.78	1.05	0.10	1.39	0.03	0.06	1.94
DL	2.20	0.20	44.9	27.0	0.20	0.10	0.10	0.10	0.10	-	25.33

Notes: MK – Metakaolin; DL - Dolomitic lime; LOI - Loss on ignition.

The metakaolin used in this study has a SiO<sub>2</sub>/Al<sub>2</sub>O<sub>3</sub> molar ratio of 3.80. Although opinions about the ideal SiO<sub>2</sub>/Al<sub>2</sub>O<sub>3</sub> ratio differ among researchers, the SiO<sub>2</sub>/Al<sub>2</sub>O<sub>3</sub> ratio in this study is within the acceptable range (between 1.92 and 5.59) presented in the study by Jindal et al. [15] for the production of metakaolin-based geopolymers. XRD patterns of MK (Figure 1) showed crystalline phases of anatase, quartz, and muscovite. These materials are impurities of MK. In addition, the XRD of MK showed an amorphous structure between 15 and 35° 2θ, which is characteristic of the material after the calcination process [15]. However, the presence of kaolinite was not observed. Kaolinite is a raw material used in the production of metakaolin. Therefore, the calcination process was efficient and allowed complete dehydroxylation of the kaolinite mineral phase during calcination. In addition, the XRD pattern of the MK (Figure 1) suggests that the crystalline phases of the MK remained inert in the matrix. The high crystallinity does not allow the complete dissolution of the MK by the activating solution in the geopolymerization process [26]. This is not necessarily a problem because these crystalline phases of MK can act as a filler and improve the densification of the matrix [27]

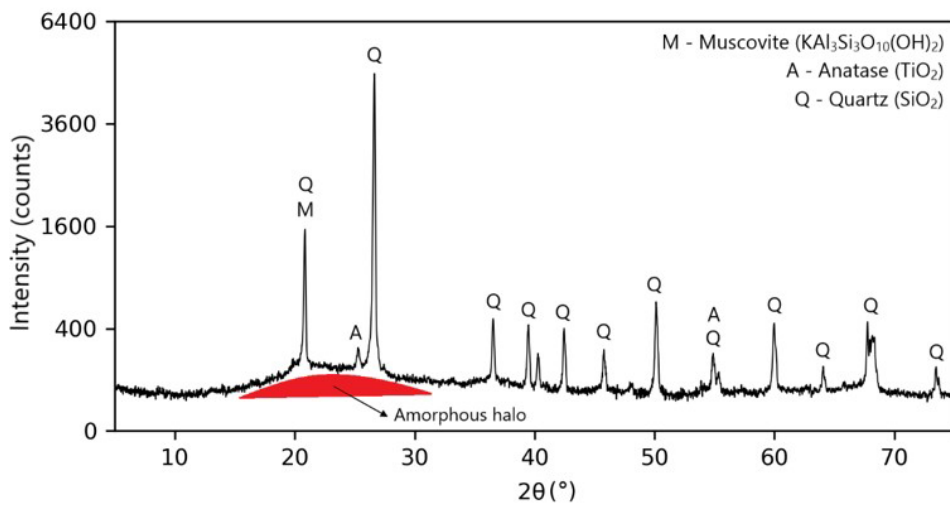


**Figure 1.** XRD pattern of the metakaolin (MK).

The XRD analysis of the DL (Figure 2) showed crystalline phases of portlandite (Ca(OH)<sub>2</sub>), brucite (Mg(OH)<sub>2</sub>), dolomite (CaMg(CO<sub>3</sub>)<sub>2</sub>), and calcite (CaCO<sub>3</sub>). The high magnesium (MgO) content identified in the XRF analysis of the DL (Table 1) and the brucite and dolomite crystalline phases identified in the XRF analysis (Figure 2) confirmed the dolomitic nature of the DL.

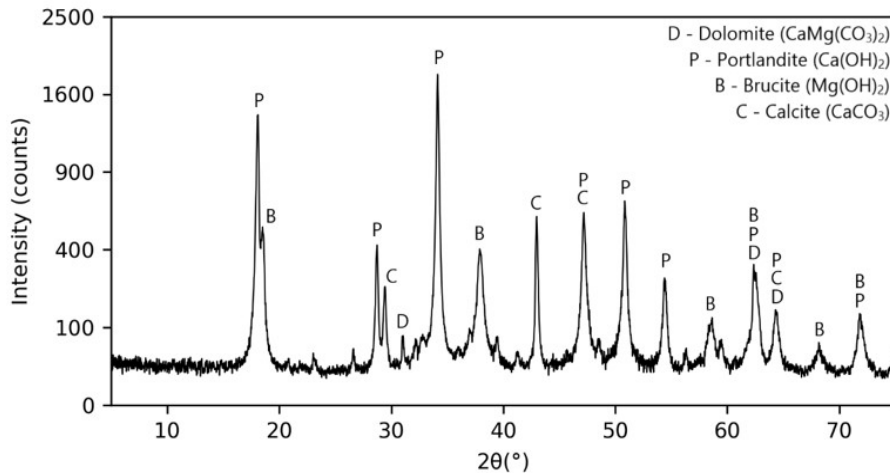


Figure 2. XRD pattern of the dolomitic lime (DL).

### 2.1.2 Activator solution

The alkaline activator used is a mixture of sodium hydroxide (SH) and sodium silicate (SS). The sodium hydroxide used is 97% pure. The sodium silicate solution used is composed of 52.75% H<sub>2</sub>O, 32.25% SiO<sub>2</sub>, and 15.0% Na<sub>2</sub>O and has an apparent density of 1572.5 kg/m<sup>3</sup>.

### 2.1.3 Mixture proportion

Table 2 shows the mixtures of the geopolymers produced. Five mixtures were prepared with 0.0%, 2.5%, 5.0%, 7.5%, and 10.0% incorporation of DL on the total mass of solids in the mixture. The reference mixture (G0.0) was developed according to previous tests and the optimal molar ratios of Na<sub>2</sub>O/Al<sub>2</sub>O<sub>3</sub> and H<sub>2</sub>O/Na<sub>2</sub>O identified by Riahi et al. [14] and Lahoti et al. [28]. According to Riahi et al. [14], these molar ratios have a significant influence on the compressive strength of geopolymers. Therefore, the incorporation of DL does not affect the Na<sub>2</sub>O/Al<sub>2</sub>O<sub>3</sub> and H<sub>2</sub>O/Na<sub>2</sub>O molar ratios used in this study.

Table 2. Mixture proportions.

Code	MK (kg)	DL (kg)	SS (kg)	SH (kg)	Water (kg)	water/solids	Na <sub>2</sub> O/ Al <sub>2</sub> O <sub>3</sub>	H <sub>2</sub> O/ Na <sub>2</sub> O
G0.0	100.0	-	62.9	8.4	21.7	0.40	0.9	12.0
G2.5	100.0	3.5	62.9	8.4	21.7	0.39	0.9	12.0
G5.0	100.0	7.6	62.9	8.4	21.7	0.38	0.9	12.0
G7.5	100.0	11.2	62.9	8.4	21.7	0.37	0.9	12.0
G10.0	100.0	15.3	62.9	8.4	21.7	0.36	0.9	12.0

Notes: MK - Metakaolin; DL - Dolomitic lime; SS - Sodium silicate; SH - Sodium hydroxide.

Silica sand (mesh -70) with a specific gravity of 2.65 g/cm<sup>3</sup> was used as a filler and as a potential means of preventing drying shrinkage cracking in the geopolymer. The ratio of the mass of the geopolymer paste to the mass of the silica sand was equal to 1.0. Incorporating sand particles into the geopolymer mixture can significantly reduce the relative shrinkage from 2% to approximately zero, which contributes to improving the compressive strength of geopolymers, as discussed by Riahi et al. [14].

### 2.1.4 Sample preparation and curing

Figure 3 shows the steps in the preparation and curing process of the geopolymer mixtures. Initially, the sodium hydroxide was diluted in water and the resulting solution was mixed with the sodium silicate. After that, the alkaline activator remained at rest for 24 hours to reach thermal equilibrium with the environment. The geopolymer pastes were then prepared by mixing the MK and DL with the alkaline activator in a mortar mixer for 3 minutes. Finally, the silica sand was incorporated into the mixture and the material was mixed for another 3 minutes.



**Figure 3.** Steps in the preparation of geopolymer mixtures.

The geopolymer specimens were cast in cubic ( $50 \times 50 \times 50$  mm) plastic molds. First, the specimens were allowed to cure for 24 hours at a room temperature of  $(23 \pm 2)$  °C. After this time, the specimens were removed from the molds. To prevent early water loss from the specimens, the specimens were sealed with polypropylene film. This was necessary because early water loss during geopolymerization reactions can reduce the compressive strength of geopolymers [29]–[31]. Finally, the specimens were cured at room temperature  $(23 \pm 2)$  °C until the age of the tests performed.

## 2.2 Methods

### 2.2.1 Compressive strength

The compressive strength of the geopolymer mixtures was determined at 1, 7, and 28 days of age, according to ASTM C109 [32]. Four specimens of  $50 \times 50 \times 50$  mm were used for each geopolymer mixture at each age. The test was performed in a 1000 kN capacity hydraulic press at  $(0.90 \pm 0.05)$  MPa/s load rate. Results were statistically analyzed using analysis of variance and Tukey's test at 5% significance.

### 2.2.2 Immersion Absorption and Void Index

Water immersion absorption and void index tests were carried out according to ASTM C140 [33] on three specimens ( $50 \times 50 \times 50$  mm) at an age of 28 days for each of the geopolymer mixtures produced. The saturated mass immersed in water ( $M_i$ ) of the specimens was determined using a hydrostatic balance. After this, the specimens were then removed from the water, drained and the saturated mass ( $M_s$ ) was determined using a digital balance. The dry mass ( $M_d$ ) was then determined by placing the samples in an oven at a temperature of  $(110 \pm 5)$  °C until a constant mass was reached. From the determination of these parameters, the water absorption by immersion and the voids index of the prepared geopolymer mixtures were determined.

### 2.2.3 Microstructural analysis

The chemical composition of MK and DL was determined by X-ray fluorescence (XRF) analysis performed on a Panalytical X-ray spectrometer, model Axios Max, equipped with a 4 kV rhodium tube. The mineralogical composition of MK, DL, and the geopolymer pastes (without silica sand incorporation) was determined by X-ray diffraction (XRD) analysis. After 28 days of ambient curing, the geopolymer paste samples were ground in a porcelain mortar. The ground material was sieved through a #200 mesh sieve. The resulting powder was dried in an oven at 40°C. Analyses were performed using Rigaku Mini Flex 600 equipment. A copper radiation source ( $\text{Cu K}\alpha$ ,  $\lambda = 1.54$  Å) was used and the anticathode voltage was 40 kV. The XRD analysis was performed by scanning at  $2\theta$  angles ranging from 5° to 75°.

The scanning speed was 3°/min. The microstructure of the geopolymer pastes (without silica sand incorporation) was analyzed using a scanning electron microscope (SEM), model TESCAN VEGA3, operated in high vacuum mode with an acceleration voltage of 15 kV. Energy dispersive spectroscopy (EDS) analyses were performed using an energy-dispersive X-ray spectrometer (Oxford Instruments).

### 3. RESULTS AND DISCUSSIONS

Figure 4 shows the XRD analyses performed on the produced geopolymer mixtures. The crystalline phases of quartz, anatase, and muscovite were identified in all the produced geopolymer mixtures. These crystalline phases are impurities of MK (Figure 1) and remain inert in the geopolymer matrix because they were not dissolved by the alkaline activator. This shows that the alkaline activator was not able to dissolve the crystalline impurities of MK, which remained inert in the matrix of the produced geopolymers. However, the portlandite crystalline phase of DL (Figure 2) was not identified in the XRD analyses of the produced geopolymer mixtures (Figure 4). This indicates that portlandite is reactive in geopolymer mixtures and was completely consumed during geopolymerization.

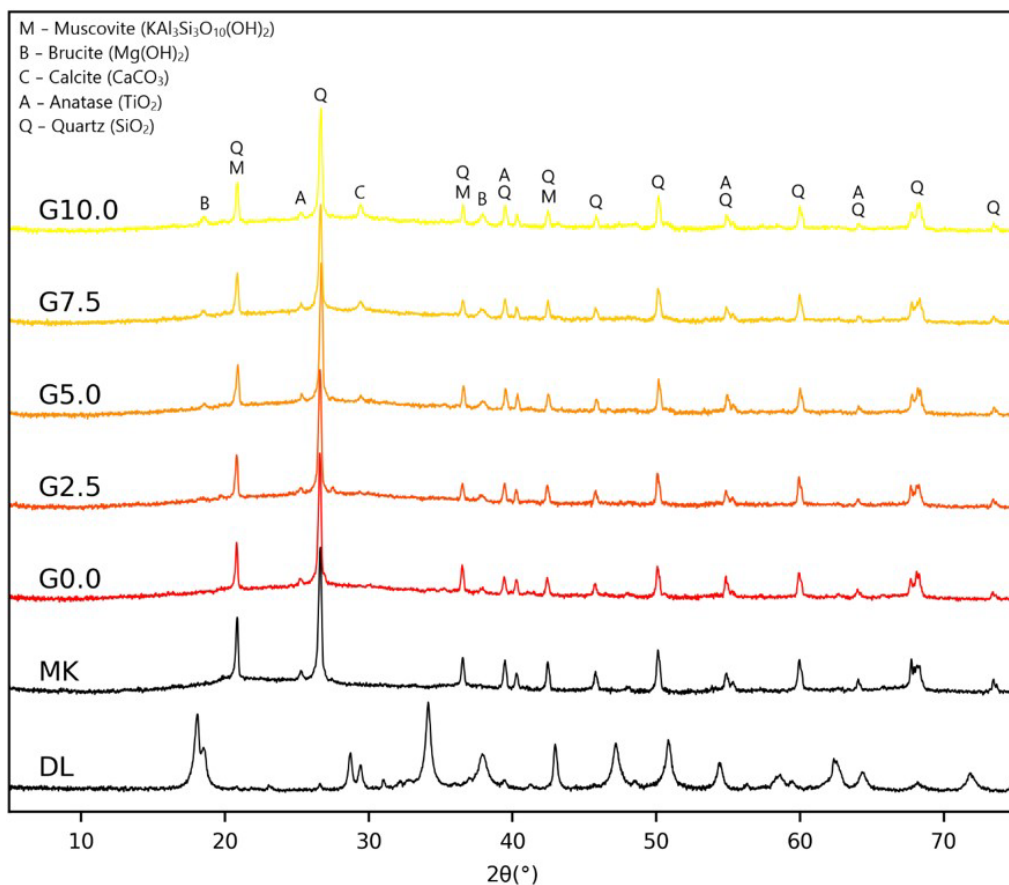


Figure 4. XRD of the metakaolin (MK), dolomitic lime (DL), and geopolymer mixtures at 28 days of age.

Through XRD analysis, Mijarsh et al. [20] observed that there was no  $\text{Ca(OH)}_2$  remaining in their geopolymer mixtures with the incorporation of this material. Similarly, Walkley et al. [34] observed no  $\text{Ca(OH)}_2$  peaks in XRD analyses of metakaolin-based geopolymer mixtures with  $\text{Ca(OH)}_2$  incorporation after 28 days of ambient curing. Yang et al. [4] also noted that portlandite was completely consumed when incorporated in small amounts in the geopolymer mixtures. Si et al. [18] also observed that  $\text{Ca(OH)}_2$  can be completely consumed during the C-S-H phase formation process in the metakaolin-based geopolymer. Therefore, discussions in the literature support the hypothesis that the portlandite from DL was completely dissolved by the alkaline activator and participated in the geopolymerization reactions.

Consequently, the compressive strength of the mixtures was affected (Figure 5). The dissolution of portlandite ( $\text{Ca(OH)}_2$ ) provided calcium to the geopolymer matrix, allowing the formation of calcium aluminosilicate gels. Figure 5 shows the compressive strength of the geopolymer mixtures produced at 1, 7, and 28 days of age. The compressive strength of the mixtures with DL incorporation (G2.5, G5.0, G7.5, and G10.0) was higher than the compressive strength of the reference mixture (G0.0) at all ages.

Furthermore, the amount of calcium available in the geopolymeric system directly influences the type of gel formed. Garcia-Lodeiro et al. [35] indicated that high calcium availability produced more stable C-A-S-H and  $\text{C}_2\text{ASH}_8$  gel phases, while low calcium availability produced an amorphous (N, C)-A-S-H gel. Similarly, Luo et al. [36] observed that the availability of calcium directly affected the composition of the formed gels. When calcium availability is limited, an N-A-S-H gel with partial calcium uptake is formed, preserving the 3D structure of the geopolymer. As a result, two hydrated gels, C-(N)-ASH type gel and N-(C)-ASH type gel, are separately developed into a hybrid binder. Therefore, the incorporation of DL into the geopolymer matrix caused the formation of different types of calcium aluminosilicate gels due to the variation of calcium availability in the geopolymer matrix. However, the likely products of portlandite during geopolymerization reactions are calcium silicate hydrate (C-S-H) or calcium aluminosilicates (C-A-S-H) in amorphous or poorly ordered form, which is difficult to identify by XRD [2]. Therefore, the results of the other microstructural analysis tests (SEM/EDS) need to be discussed to confirm this hypothesis.

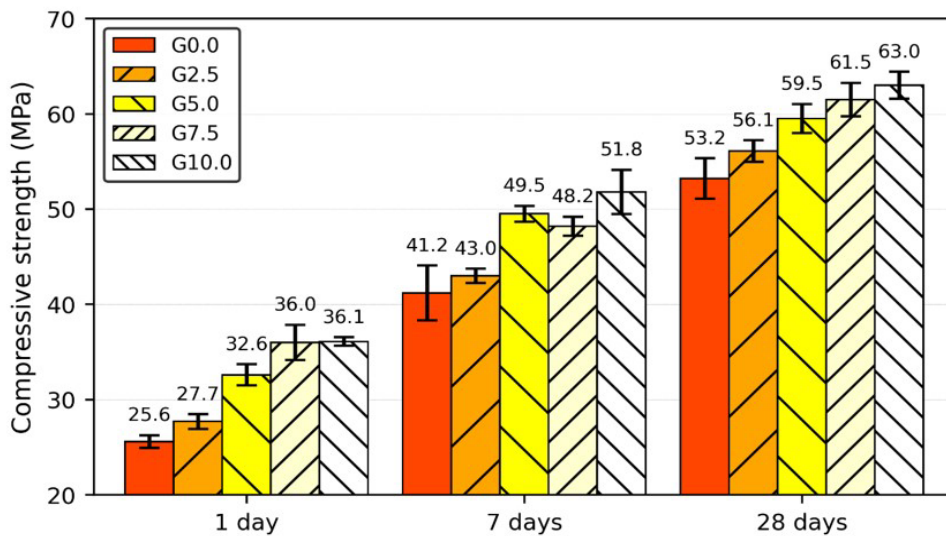
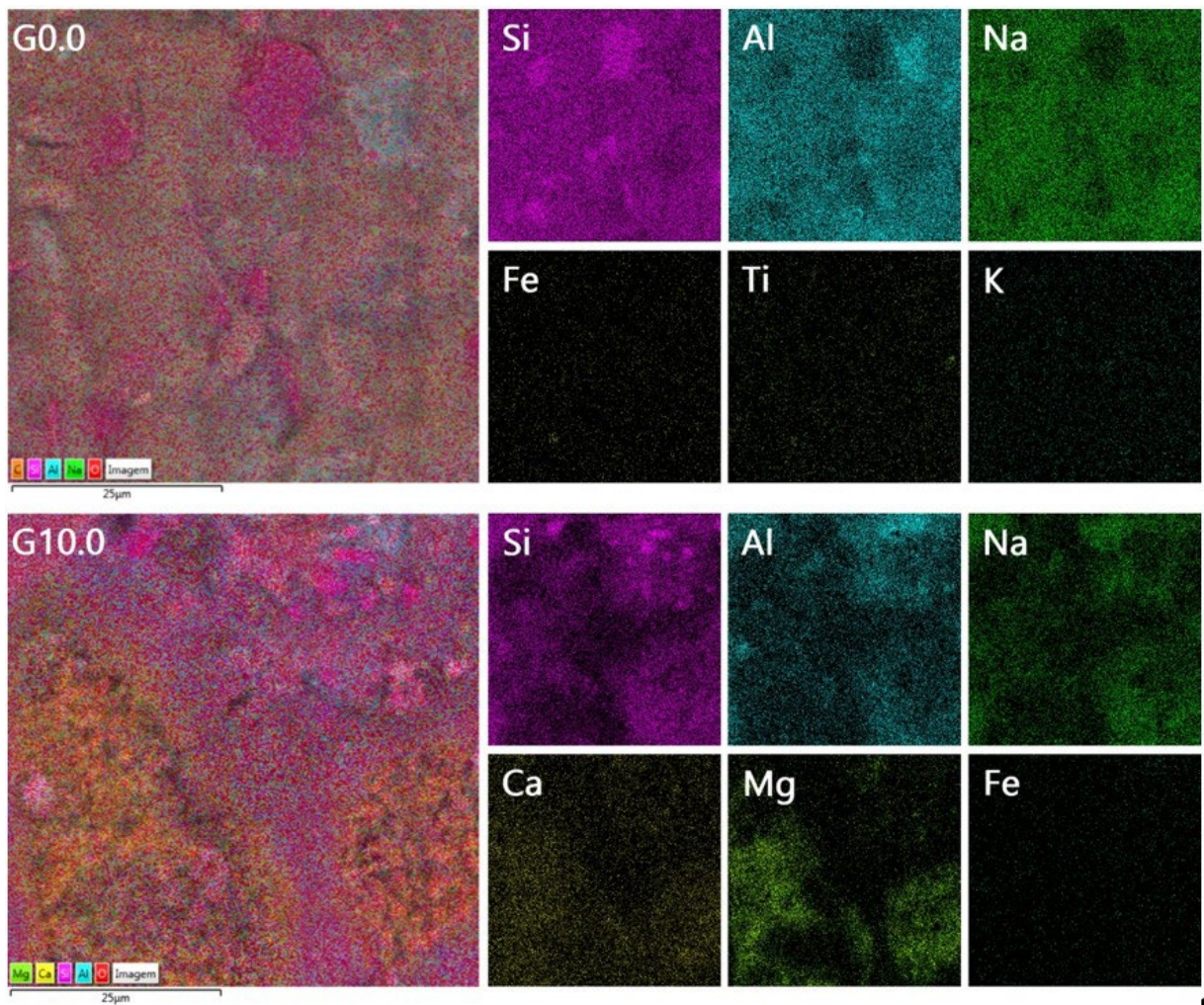


Figure 5. Compressive strength of geopolymer mixtures at 1, 7, and 28 days.

Statistical analysis of variance and Tukey's test showed that the incorporation of DL into the geopolymer caused a significant increase in compressive strength of 5.5%, 11.9%, 15.8%, and 18.5% at 28 days in G2.5, G5.0, G7.5, and G10.0, respectively, compared to the reference mixture (G0.0). However, although DL incorporation contributes to the increase in compressive strength, there is no statistically significant difference between the compressive strength of G7.5 and G10.0 at 28 days of age. Therefore, considering the cost of DL incorporation, the optimum content for incorporation of DL into the geopolymer was 7.5%.

The formation of C-S-H and C-A-S-H gels together with N-A-S-H gel in the geopolymer matrix due to the incorporation of portlandite from DL can explain the increase in compressive strength. The formation of C-S-H and C-A-S-H gels together with N-A-S-H gel in the geopolymer matrix [2], [4], [5], [7], [17]–[22], [25] produces better mechanical properties in the geopolymer due to matrix refinement [23]. This hypothesis was confirmed by the analysis of the microstructure of the materials as shown in Figure 6. The chemical element distribution maps obtained by SEM/EDS (Figure 6) of the G0.0 and G10.0 mixtures confirm the results of the XRD analyses (Figure 4).



**Figure 6.** SEM/EDS maps of the G0.0 and G10.0 mixtures.

The N-A-S-H gel was the phase formed from the geopolymerization in the G0.0 mixture. In both mixtures (G0.0 and G10.0), regions with high concentrations of silicon and low concentrations of aluminum and sodium were identified, corresponding to the quartz crystalline phase of MK (Figure 1), which was not dissolved by the alkaline activator. This confirms that the quartz crystalline phases have chemical stability and are not dissolved by the alkaline activator. Thus, SEM/EDS analyses (Figure 6) show that the high crystallinity of the precursor (Figure 1) is still present in the geopolymer matrix. This also confirms the presence of quartz crystalline phases identified in the XRD analyses of the geopolymer pastes (Figure 4). In addition, the calcium dissolved by the alkaline activator, which comes from the portlandite of DL (Figure 2), was uniformly distributed in the G10 mixture. This indicates that the calcium is part of the geopolymer matrix due to the coexistence of the C-A-S-H gel together with the N-A-S-H geopolymer gel. Garcia-Lodeiro et al. [35] showed that the presence of calcium modifies N-A-S-H gel favoring the C-A-S-H formation in a medium with high pH (>12). Similarly, Temuujin et al. [2] observed that calcium was homogeneously distributed inside of the matrix when analyzing the microstructure of fly ash-based geopolymer matrix with CaO and Ca(OH)<sub>2</sub> incorporation. As the calcium incorporation values are small, around 4.7% of the mass of solids for G10.0, calcium is predicted to be preferentially adsorbed and sodium will only be retained if there is insufficient calcium, which leads to the Ca<sup>2+</sup> ions from the dissolution of DL to interact with the N-A-S-H gel to form a (N, C)-A-S-H gel [20].

The high magnesium regions (Figure 6) show that magnesium precipitation has occurred in some regions of G10.0 due to the presence of Mg(OH)<sub>2</sub> (brucite) precipitates. However, the magnesium is homogeneously distributed in the geopolymeric matrix outside of the brucite precipitation region. This indicates that the brucite from the DL was partially dissolved by the alkaline activators and the dissolved part was incorporated into the geopolymer matrix.

Thus, the homogeneously distributed magnesium in the geopolymer matrix indicates the formation of a gel of hydrated magnesium and sodium aluminosilicates. Hu et al. [37] observed that  $Mg^{2+}$  ions can be incorporated into the matrix during geopolymerization reactions. In the evaluation of geopolymers produced with high magnesium content ground ferronickel slag and fly ash, Kuri et al. [38] observed that the magnesium reacted with the Si-O-Si, Al-O-Al, or Al-O-Si bonds in the geopolymerization reactions and developed a magnesium-sodium aluminosilicate hydrate (N-M-A-S-H) gel. This resulted in higher compressive strength in the mixtures containing ground ferronickel slag. Similarly, Yang et al. [39] identified that the main phases formed in geopolymers with nickel slag are a class of sodium-magnesium-aluminosilicate gels. Therefore, the distribution of magnesium in the geopolymer matrix (Figure 7) indicates the formation of hydrated sodium magnesium aluminosilicate (N-M-A-S-H), which also contributes to the increased compressive strength (Figure 5) of geopolymers produced with DL incorporation.

Thus, C-A-S-H and N-M-A-S-H gels coexisted with the N-A-S-H gel in the mixtures with DL incorporation. This confirms the hypothesis that the increase in compressive strength (Figure 5) with increasing DL incorporation is due to the formation of these gels during geopolymerization. Therefore, the presence of these gels in the geopolymer matrix resulted in matrix refinement, which was also observed in the void index (Figure 7a) and absorption (Figure 7b) tests.

According to Figure 7, both results showed that the void index (Figure 7a) and the immersion absorption (Figure 7b) of the geopolymers were reduced as a function of increasing DL incorporation. Statistical analysis shows that DL incorporation caused a significant reduction in void index and absorption of G2.5, G5.0, G7.5, and G10.0 compared to G0.0.

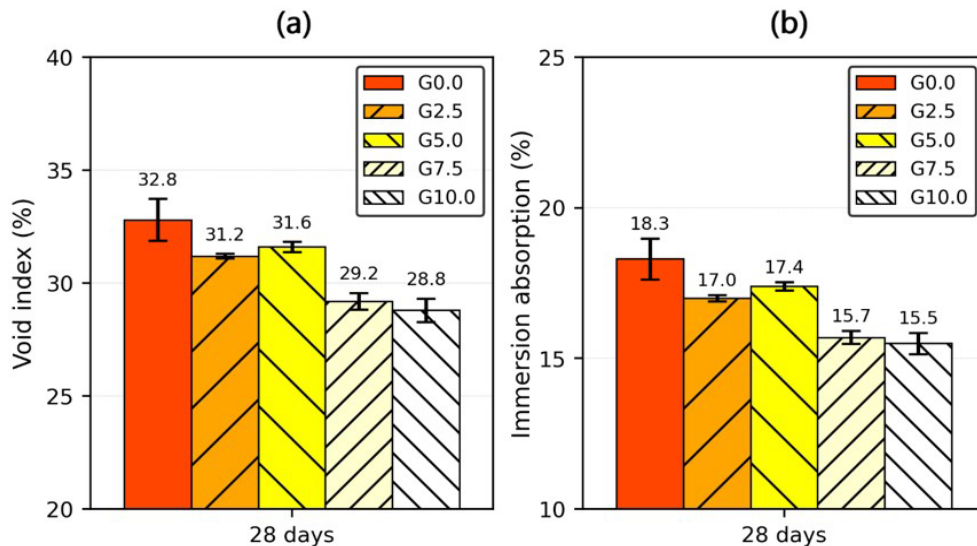
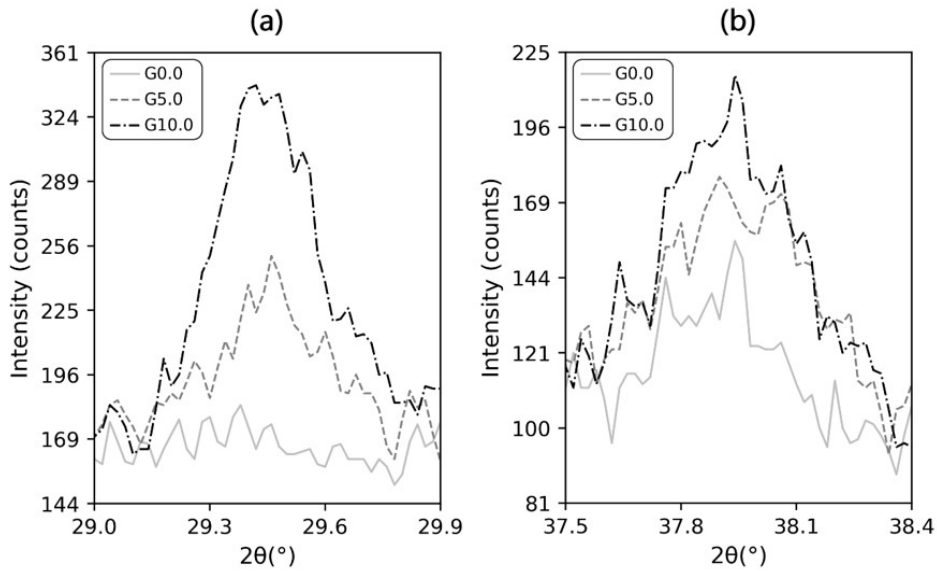


Figure 7. Results of the (a) voids index and (b) immersion absorption of the geopolymers.

However, similar to the behavior observed in the compressive strength test, there is no statistically significant difference between the void content and the absorption by immersion obtained between G7.5 and G10.0 at 28 days of age. Therefore, these results converge with the results obtained in the compressive strength test (Figure 5) and confirm the hypothesis that the densification of the geopolymeric matrix occurred due to the formation of C-A-S-H and N-M-A-S-H gels together with the N-A-S-H gel.

In contrast, crystalline phases of brucite and calcite were identified in the mixtures with DL incorporation (Figure 4). Thus, these materials derived from the DL (Figure 2) remained precipitated in the geopolymer matrix. This indicates that the brucite and calcite were not dissolved or were partially dissolved by the alkaline activator. Figure 8 shows the XRD analyses of the G0.0, G5.0, and G10.0 mixtures in the region of the highest intensity peak of calcite ( $29.356^\circ$ , PDF: 00-001-0837) and brucite ( $37.984^\circ$ , PDF: 01-083-0114). For both materials, there is an increase in the peak of higher intensity as a function of increasing DL incorporation content in the geopolymer. Therefore, the precipitation of calcite and brucite in the geopolymer matrix increases with the DL incorporation.



**Figure 8.** XRD of mixtures G0.0, G5.0, and G10.0 in the region of the peak of the highest intensity of (a) calcite; and (b) brucite.

Clausi et al. [3] noted that calcite grains, which were not dissolved by the alkaline activator, favor the coexistence of the C-A-S-H gel along with the N-A-S-H gel in some regions of the geopolymer matrix. This behavior is due to the high calcium content available in these regions due to calcite precipitation and is consistent with the result identified by Garcia-Lodeiro et al. [35], who observed the formation of the C-A-S-H gel in materials with high calcium contents. Thus, calcite precipitation may be beneficial for the geopolymeric matrix due to the formation of calcium aluminosilicate gels in the region of material precipitation. In addition, dolomite decomposes in an alkaline medium, which favors the formation of brucite [3]. Therefore, the dolomite identified in the XRD analysis of DL (Figure 2) may have converted to brucite, because this material was not identified in the XRD analyses of the geopolymer mixtures with DL incorporation (Figure 4). However, there are no studies in the literature on the effects of brucite precipitation in the geopolymer matrix, which proves an important innovation for this article. Figure 9a shows the precipitation of brucite in the matrix of the G10 mixture identified by SEM.

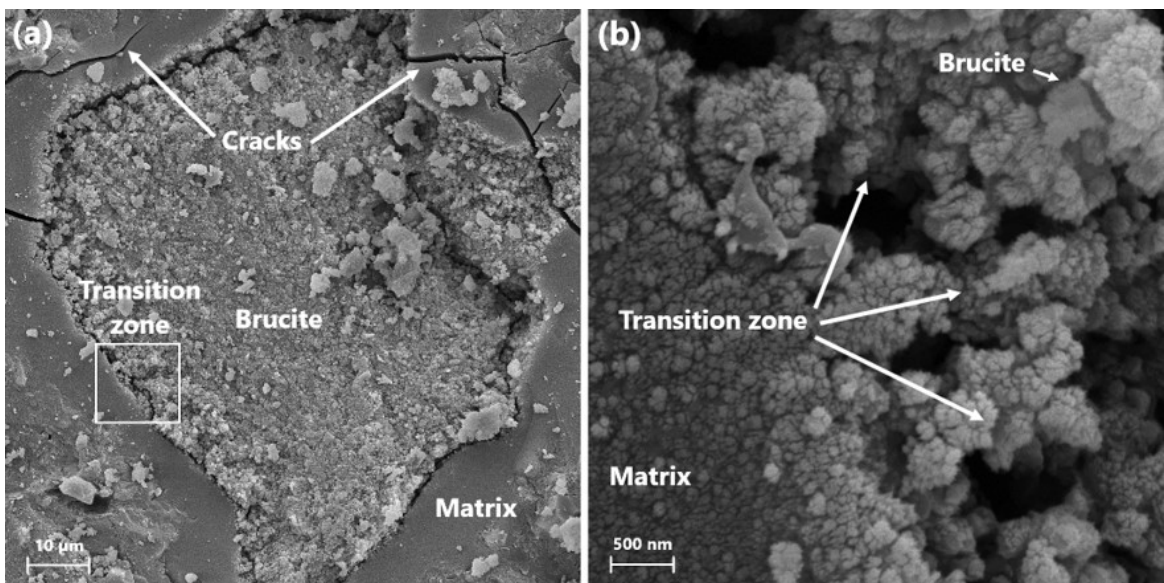


**Figure 9.** SEM of G10.0: (a) brucite precipitation in the matrix; (b) transition zone between matrix and precipitated brucite.

This confirmed the results of the XRD (Figure 8b) and SEM/EDS (Figure 6) analyses. The material was not completely dissolved by the alkaline activator and remained in the form of an inert precipitate in the geopolymer matrix. Figure 9b shows that the region of the geopolymer matrix has a fine and more homogeneous microstructure, while the region of the brucite precipitation has a heterogeneous structure. Furthermore, the transition zone (Figure 9b) between the matrix and the precipitated brucite shows that there was no satisfactory adhesion between the materials, which may have resulted in a higher porosity than the rest of the matrix. Consequently, this porous transition zone may affect the mechanical properties of the produced geopolymers. This may explain the fact that mixtures G7.5 and G10.0 showed statistically equal values for compressive strength (Figure 5), void index (Figure 7a), and absorption per immersion (Figure 7b) after 28 days of age. Thus, the increase in compressive strength (Figure 5) due to the formation of C-A-S-H and N-M-A-S-H gels (Figure 6) may not be sufficient to compensate for the loss in compressive strength (Figure 5) due to the precipitation of brucite in the geopolymer matrix. In contrast, Figure 10 shows that the quartz particles exhibit excellent bonding with the geopolymer matrix.

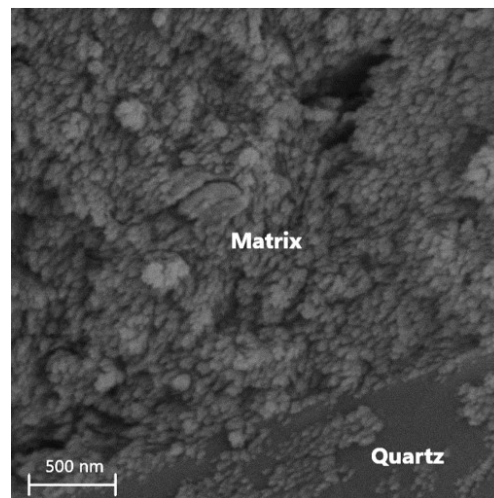


**Figure 10.** SEM of the transition zone between the geopolymer matrix and the quartz from metakaolin in the G10.0 mixture.

This is consistent with the fact that quartz particles can significantly control shrinkage and improve the mechanical properties of the produced geopolymers [14], [29]. As the dissolution of quartz by the alkaline solution is incipient, quartz particles act as a filler and densify the microstructure of the geopolymer [14], [40]. Therefore, despite being considered an impurity in MK (Figure 1), quartz particles can contribute to improving the mechanical strength of geopolymers. Figure 10 also shows the formation of a gel in the geopolymer matrix characterized by a homogeneous microstructure. This explains why the C-A-S-H, N-M-A-S-H, and N-A-S-H gels were not detected by XRD analysis (Figure 4), since these materials are mostly amorphous and have no defined geometric shape.

## 5. CONCLUSIONS

In this study, the effects of DL incorporation on the mechanical properties and microstructure of MK-based geopolymer were investigated. Based on the results of the tests and analyses performed, it was concluded that:

- Portlandite ( $\text{Ca}(\text{OH})_2$ ) was completely consumed and brucite ( $\text{Mg}(\text{OH})_2$ ) was partially consumed during the geopolymerization. This allowed the coexistence of the C-A-S-H and N-M-A-S-H gels in the geopolymer matrix together with the N-A-S-H gel.
- The coexistence of the C-A-S-H and N-M-A-S-H gels together with the N-A-S-H gel explains the increase in compressive strength in the geopolymer mixtures with DL incorporation when compared to the reference mixture without DL incorporation. Also, the results of the void index and the immersion absorption tests corroborate with the results of the compressive strength tests. Thus, it was possible to obtain 63.0 MPa compressive strength in mixture G10.0 at 28 days, which corresponds to an 18.4% increase over the reference mixture without DL (G0.0).

- The transition zone between the geopolymer matrix and the precipitated brucite ( $Mg(OH)_2$ ) indicated that a satisfactory adhesion between the materials did not occur. Thus, the weak bond between the two materials may have compromised the compressive strength of the geopolymer. This may have limited the increase in compressive strength because mixtures with 7.5% and 10.0% of DL incorporation showed statistically equal compressive strengths.
- XRD and SEM/EDS analyses showed that the quartz particles act as a filler and densify the microstructure of the geopolymer due to the incipient dissolution of the quartz particles by the alkaline solution. Thus, although considered an impurity of metakaolin, quartz particles can contribute to the increased mechanical strength of geopolymers due to the excellent transition zone between the geopolymer matrix and the quartz.
- Finally, the results of the tests performed showed that the incorporation of DL was effective since it was possible to significantly improve the mechanical strength of metakaolin-based geopolymers with a material of relatively low cost. However, studies on the evolution of the gels formed by the incorporation of DL at later ages are necessary to provide information on the durability of these materials.

## ACKNOWLEDGEMENTS

The authors would like to thank the Central Analysis Laboratory of the Federal Technological University of Parana (UTFPR), the Laboratory of Mineral and Rock Analysis (LAMIR), the Center of Electron Microscopy of the UFPR (CME/UFPR), and the Postgraduate Program of Civil Engineering (PPGEC) of the Federal University of Parana (UFPR). The authors also thank the Brazilian Federal Agency for the Support and Evaluation of Graduate Education (CAPES), the National Council for Scientific and Technological Development (CNPQ), the Araucária Foundation (Grant number 044/2020), and the Federal Institute of Santa Catarina (IFSC) for their support in conducting this study.

## REFERENCES

- [1] N. B. Singh and B. Middendorf, "Geopolymers as an alternative to Portland cement: an overview," *Constr. Build. Mater.*, vol. 237, pp. 117455, Mar 2020, <http://dx.doi.org/10.1016/j.conbuildmat.2019.117455>.
- [2] J. Temuujin, A. van Riessen, and R. Williams, "Influence of calcium compounds on the mechanical properties of fly ash geopolymer pastes," *J. Hazard. Mater.*, vol. 167, no. 1–3, pp. 82–88, Aug 2009, <http://dx.doi.org/10.1016/j.jhazmat.2008.12.121>.
- [3] M. Clausi, A. M. Fernández-Jiménez, A. Palomo, S. C. Tarantino, and M. Zema, "Reuse of waste sandstone sludge via alkali activation in matrices of fly ash and metakaolin," *Constr. Build. Mater.*, vol. 172, pp. 212–223, May 2018, <http://dx.doi.org/10.1016/j.conbuildmat.2018.03.221>.
- [4] J. Yang et al., "An efficient approach for sustainable fly ash geopolymer by coupled activation of wet-milling mechanical force and calcium hydroxide," *J. Clean. Prod.*, vol. 372, pp. 133771, Oct 2022, <http://dx.doi.org/10.1016/j.jclepro.2022.133771>.
- [5] B. Ma et al., "The influence of calcium hydroxide on the performance of MK-based geopolymer," *Constr. Build. Mater.*, vol. 329, pp. 127224, Apr 2022, <http://dx.doi.org/10.1016/j.conbuildmat.2022.127224>.
- [6] A. Albidah, A. S. Alqarni, H. Abbas, T. Almusallam, and Y. Al-Salloum, "Behavior of metakaolin-based geopolymer concrete at ambient and elevated temperatures," *Constr. Build. Mater.*, vol. 317, pp. 125910, Jan 2022, <http://dx.doi.org/10.1016/j.conbuildmat.2021.125910>.
- [7] B. Kim, S. Lee, C.-M. Chon, and S. Cho, "Setting behavior and phase evolution on heat treatment of metakaolin-based geopolymers containing calcium hydroxide," *Materials*, vol. 15, no. 1, pp. 194, Dec 2021, <http://dx.doi.org/10.3390/ma15010194>.
- [8] F. Farooq et al., "Geopolymer concrete as sustainable material: a state of the art review," *Constr. Build. Mater.*, vol. 306, pp. 124762, Nov 2021, <http://dx.doi.org/10.1016/j.conbuildmat.2021.124762>.
- [9] A. Danish et al., "Sustainability benefits and commercialization challenges and strategies of geopolymer concrete: a review," *J. Build. Eng.*, vol. 58, pp. 105005, Oct 2022, <http://dx.doi.org/10.1016/j.jobbe.2022.105005>.
- [10] J. Zhao et al., "Eco-friendly geopolymer materials: a review of performance improvement, potential application and sustainability assessment," *J. Clean. Prod.*, vol. 307, pp. 127085, Jul 2021, <http://dx.doi.org/10.1016/j.jclepro.2021.127085>.
- [11] F. B. Witzke, N. A. M. Beltrame, C. Angulski da Luz, and R. A. Medeiros-Junior, "Abrasion resistance of metakaolin-based geopolymers through accelerated testing and natural wear," *Wear*, vol. 530–531, pp. 204996, Oct 2023, <http://dx.doi.org/10.1016/j.wear.2023.204996>.
- [12] A. Hassan, M. Arif, and M. Shariq, "Use of geopolymer concrete for a cleaner and sustainable environment: a review of mechanical properties and microstructure," *J. Clean. Prod.*, vol. 223, pp. 704–728, Jun 2019, <http://dx.doi.org/10.1016/j.jclepro.2019.03.051>.
- [13] Y. H. M. Amran, R. Alyousef, H. Alabduljabbar, and M. El-Zeadani, "Clean production and properties of geopolymer concrete: A review," *J. Clean. Prod.*, vol. 251, pp. 119679, Apr 2020, <http://dx.doi.org/10.1016/j.jclepro.2019.119679>.

- [14] S. Riahi, A. Nemati, A. R. Khodabandeh, and S. Baghshahi, "The effect of mixing molar ratios and sand particles on microstructure and mechanical properties of metakaolin-based geopolymers," *Mater. Chem. Phys.*, vol. 240, pp. 122223, Jan 2020, <http://dx.doi.org/10.1016/j.matchemphys.2019.122223>.
- [15] B. B. Jindal, T. Alomayri, A. Hasan, and C. R. Kaze, "Geopolymer concrete with metakaolin for sustainability: a comprehensive review on raw material's properties, synthesis, performance, and potential application," *Environ. Sci. Pollut. Res. Int.*, vol. 30, no. 10, pp. 25299–25324, Jan 2022, <http://dx.doi.org/10.1007/s11356-021-17849-w>.
- [16] M. T. Marvila, A. R. G. Azevedo, and C. M. F. Vieira, "Reaction mechanisms of alkali-activated materials," *Rev. IBRACON Estrut. Mater.*, vol. 14, no. 3, e14309, 2021, <http://dx.doi.org/10.1590/s1983-41952021000300009>.
- [17] K. M. L. Alventosa and C. E. White, "The effects of calcium hydroxide and activator chemistry on alkali-activated metakaolin pastes," *Cement Concr. Res.*, vol. 145, pp. 106453, Jul 2021, <http://dx.doi.org/10.1016/j.cemconres.2021.106453>.
- [18] R. Si, S. Guo, and Q. Dai, "Influence of calcium content on the atomic structure and phase formation of alkali-activated cement binder," *J. Am. Ceram. Soc.*, vol. 102, no. 3, pp. 1479–1494, Mar 2019, <http://dx.doi.org/10.1111/jace.15968>.
- [19] X. Chen, A. Sutrisno, and L. J. Struble, "Effects of calcium on setting mechanism of metakaolin-based geopolymer," *J. Am. Ceram. Soc.*, vol. 101, no. 2, pp. 957–968, Feb 2018, <http://dx.doi.org/10.1111/jace.15249>.
- [20] M. J. A. Mijarsh, M. A. Megat Johari, and Z. A. Ahmad, "Compressive strength of treated palm oil fuel ash based geopolymer mortar containing calcium hydroxide, aluminum hydroxide and silica fume as mineral additives," *Cement Concr. Compos.*, vol. 60, pp. 65–81, Jul 2015, <http://dx.doi.org/10.1016/j.cemconcomp.2015.02.007>.
- [21] H. Madani, A. A. Ramezani-pour, M. Shahbazinia, and E. Ahmadi, "Geopolymer bricks made from less active waste materials," *Constr. Build. Mater.*, vol. 247, pp. 118441, Jun 2020, <http://dx.doi.org/10.1016/j.conbuildmat.2020.118441>.
- [22] X. Zhao, C. Liu, L. Zuo, L. Wang, Q. Zhu, and M. Wang, "Investigation into the effect of calcium on the existence form of geopolymerized gel product of fly ash based geopolymers," *Cement Concr. Compos.*, vol. 103, pp. 279–292, Oct 2019, <http://dx.doi.org/10.1016/j.cemconcomp.2018.11.019>.
- [23] W. Huo, Z. Zhu, H. Sun, B. Ma, and L. Yang, "Development of machine learning models for the prediction of the compressive strength of calcium-based geopolymers," *J. Clean. Prod.*, vol. 380, pp. 135159, Dec 2022, <http://dx.doi.org/10.1016/j.jclepro.2022.135159>.
- [24] Y. Lv, J. Qiao, W. Han, B. Pan, X. Jin, and H. Peng, "Modification effect of Ca(OH)<sub>2</sub> on the carbonation resistance of fly ash-metakaolin-based geopolymer," *Materials*, vol. 16, no. 6, pp. 2305, Mar 2023, <http://dx.doi.org/10.3390/ma16062305>.
- [25] Y. Hu et al., "Investigation into the influence of calcium compounds on the properties of micropore-foamed geopolymer," *J. Build. Eng.*, vol. 45, pp. 103521, Jan 2022, <http://dx.doi.org/10.1016/j.jobbe.2021.103521>.
- [26] L. N. Tchadjé et al., "Potential of using granite waste as raw material for geopolymer synthesis," *Ceram. Int.*, vol. 42, no. 2, pp. 3046–3055, Feb 2016., <http://dx.doi.org/10.1016/j.ceramint.2015.10.091>.
- [27] A. G. Borçato, M. Thiesen, and R. A. Medeiros-Junior, "Mechanical properties of metakaolin-based geopolymers modified with different contents of quarry dust waste," *Constr. Build. Mater.*, vol. 400, pp. 132854, 2023, <http://dx.doi.org/10.1016/j.conbuildmat.2023.132854>.
- [28] M. Lahoti, P. Narang, K. H. Tan, and E.-H. Yang, "Mix design factors and strength prediction of metakaolin-based geopolymer," *Ceram. Int.*, vol. 43, no. 14, pp. 11433–11441, Oct 2017, <http://dx.doi.org/10.1016/j.ceramint.2017.06.006>.
- [29] R. Pouhet, M. Cyr, and R. Bucher, "Influence of the initial water content in flash calcined metakaolin-based geopolymer," *Constr. Build. Mater.*, vol. 201, pp. 421–429, Mar 2019, <http://dx.doi.org/10.1016/j.conbuildmat.2018.12.201>.
- [30] S. Park and M. Pour-Ghaz, "What is the role of water in the geopolymerization of metakaolin," *Constr. Build. Mater.*, vol. 182, pp. 360–370, Sep 2018, <http://dx.doi.org/10.1016/j.conbuildmat.2018.06.073>.
- [31] B. Mo, H. Zhu, X. Cui, Y. He, and S. Gong, "Effect of curing temperature on geopolymerization of metakaolin-based geopolymers," *Appl. Clay Sci.*, vol. 99, pp. 144–148, Sep 2014, <http://dx.doi.org/10.1016/j.clay.2014.06.024>.
- [32] American Society for Testing and Materials, *Standard Test Method for Compressive Strength of Hydraulic Cement Mortars (Using 2-in [50 mm] Cube Specimen)*, ASTM C109/C109M-20, 2020.
- [33] American Society for Testing and Materials, *Standard Test Methods for Sampling and Testing Concrete Masonry Units and Related Units*, ASTM C140/C140M-22, 2022.
- [34] B. Walkley, X. Ke, O. H. Hussein, S. A. Bernal, and J. L. Provis, "Incorporation of strontium and calcium in geopolymer gels," *J. Hazard. Mater.*, vol. 382, pp. 121015, Jan 2020, <http://dx.doi.org/10.1016/j.jhazmat.2019.121015>.
- [35] I. Garcia-Lodeiro, A. Palomo, A. Fernández-Jiménez, and D. E. Macphee, "Compatibility studies between N-A-S-H and C-A-S-H gels. Study in the ternary diagram Na<sub>2</sub>O–CaO–Al<sub>2</sub>O<sub>3</sub>–SiO<sub>2</sub>–H<sub>2</sub>O," *Cement Concr. Res.*, vol. 41, no. 9, pp. 923–931, Sep 2011, <http://dx.doi.org/10.1016/j.cemconres.2011.05.006>.
- [36] Y. Luo, H. J. H. Brouwers, and Q. Yu, "Understanding the gel compatibility and thermal behavior of alkali activated Class F fly ash/ladle slag: the underlying role of Ca availability," *Cement Concr. Res.*, vol. 170, pp. 107198, Aug 2023, <http://dx.doi.org/10.1016/j.cemconres.2023.107198>.

- [37] Z. Hu, M. Wyrzykowski, and P. Lura, "Estimation of reaction kinetics of geopolymers at early ages," *Cement Concr. Res.*, vol. 129, pp. 105971, Mar 2020., <http://dx.doi.org/10.1016/j.cemconres.2020.105971>.
- [38] J. C. Kuri, M. N. N. Khan, and P. K. Sarker, "Fresh and hardened properties of geopolymer binder using ground high magnesium ferro-nickel slag with fly ash," *Constr. Build. Mater.*, vol. 272, pp. 121877, Feb 2021, <http://dx.doi.org/10.1016/j.conbuildmat.2020.121877>.
- [39] T. Yang, X. Yao, and Z. Zhang, "Geopolymer prepared with high-magnesium nickel slag: characterization of properties and microstructure," *Constr. Build. Mater.*, vol. 59, pp. 188–194, May 2014, <http://dx.doi.org/10.1016/j.conbuildmat.2014.01.038>.
- [40] L. M. Costa, N. G. S. Almeida, M. Houmard, P. R. Cetlin, G. J. B. Silva, and M. T. P. Aguilar, "Influence of the addition of amorphous and crystalline silica on the structural properties of metakaolin-based geopolymers," *Appl. Clay Sci.*, vol. 215, pp. 106312, Dec 2021, <http://dx.doi.org/10.1016/j.clay.2021.106312>.

---

**Author contributions:** AGB: conceptualization, formal analysis, methodology, data curation, writing; NAMB, TAO: conceptualization, formal analysis, writing; RAMJ: conceptualization, supervision, methodology, formal analysis, writing.

**Editors:** Bruno Briseghella, Daniel Carlos Taissum Cardoso.